

A rejection-free stochastic simulation method for multivalent biomolecular interactions

Jin Yang*

*Chinese Academy of Sciences – Max Planck Society Partner Institute for Computational Biology,
Shanghai Institutes for Biological Sciences, Shanghai 200031, China*

William S. Hlavacek†

*Theoretical Division and Center for Nonlinear Studies,
Los Alamos National Laboratory, Los Alamos, NM 87545, USA*

The system-level dynamics of biomolecular interactions can be difficult to specify and simulate using methods that involve explicit specification of a chemical reaction network. Here, we present a stochastic simulation method for determining the kinetics of multivalent biomolecular interactions, which has a computational cost independent of reaction network size. The method is based on sampling a set of chemical transformation classes that characterize the interactions in a system. We apply the method to simulate multivalent ligand-receptor interaction systems. Simulation results reveal insights into ligand-receptor binding kinetics that are not available from previously developed equilibrium models.

PACS numbers: 82.20.Wt, 82.39.Rt, 82.40.Qt

Keywords: Kinetic Monte Carlo; Protein-protein interactions; Stochastic simulation algorithm; Chemical reactions; Ligand-receptor binding

I. INTRODUCTION

Biomolecular interactions, especially protein-protein interactions (PPI) in cell signaling systems, play essential roles in mediating cellular information processing and regulating cell behaviors and phenotypes. Mathematical modeling and simulation studies of the system-level dynamics of PPIs can help understand the molecular mechanisms of signal-transduction systems [1]. Stochastic simulation methods such as Gillespie’s method and its many variants rely on specifying a chemical reaction network [2]. However, constructing a reaction network, a complete list of reactions, can be a challenging task due to the vast number of chemical states induced by multivalent protein binding and multisite post-translational modification [3]. Coarse-grained models are often constructed that neglect the site-specific details of PPIs. Such simplified models are increasingly recognized as being inadequate for dissecting the molecular mechanisms of cell signaling systems, which can now be systematically interrogated using high-throughput experimental techniques that probe the dynamics of state changes of individual protein sites [4, 5, 6].

To construct models that incorporate site-specific details of PPIs, rule-based modeling approaches have been developed, which automate the model-building process by generating reaction networks from a set of reaction rules that characterize biomolecular interactions [7, 8, 9, 10]. Unfortunately, for typical cell signaling systems, re-

action networks implied by rules are of high dimension and often overwhelm conventional simulation methods. For example, two models have been reported recently in which the rules used to represent PPIs imply over 10^8 and 10^{23} chemical species [11, 12]. Exhaustive enumeration of all potential chemical states is usually unnecessary because in many cases protein copy numbers are far smaller than the number of all possible chemical states. However, the actual size and topology of a reaction network during a simulation are dynamic functions of copy numbers and reaction rates, and it is nontrivial to determine the sub-network that is relevant for a given set of parameters and initial conditions. To address this problem, rule-based kinetic Monte Carlo (KMC) methods have recently been developed for stochastic simulation of PPIs [13, 14]. The main idea behind these methods is to generate events by directly sampling a rule list instead of sampling a reaction list. When a rule is selected, the chemical transformation defined in the rule is applied to a set of randomly selected reactants. These methods do not require pre-simulation reaction-network generation.

Here, we present a rejection-free method for simulating multivalent ligand-receptor binding. In this method, each time step involves sampling a list of transformation classes and subsequently selecting molecules for reaction based on their joint probability of taking part in the sampled class. The method provides a viable way to cope with the combinatorial complexity encountered in signaling systems. It is particularly suitable for simulating biochemical systems that involve molecular assembly and aggregation, in which numerous pathways lead to the formation of vast numbers of distinct molecular complexes. We apply this method to simulate the kinetics of multivalent ligand-receptor interactions and describe a problem-specific implementation of the algorithm. We study the effects of ligand and receptor valences on ligand-induced

*To whom correspondence should be addressed. Present address: 320 Yue Yang Road, Shanghai 200031, China.; Electronic Address: yangjin@picb.ac.cn

†Department of Biology, University of New Mexico, Albuquerque, NM 87131, USA

receptor aggregation and fluctuations in the sizes of aggregates over a wide range of parameter values.

II. METHODS

General algorithm

In a chemical reaction model for PPIs, concentrations of chemical species define the state of a system that evolves in time. Here, we consider proteins to be the building blocks of chemical species, which can be constructed from knowledge of the states of proteins. A multidomain protein is characterized by a set of states and a list of bonds shared with binding partners. A protein switches its state as a result of a PPI, such as an event of binding or post-translational modification. A PPI can be defined by a transformation class (TC). A TC defines a reaction protocol for a group of protein types, which can be used to switch a protein from a source state to a target state at a specific rate. A TC effectively designates an ensemble of biochemical reactions that share common features. Fig. 1(a) shows typical biochemical transformations that can be specified by TCs. The TCs describe our knowledge and/or hypotheses about the protein interactions involved in a system. Fig. 1(b) illustrates the relationship between a set of TCs and the underlying reaction network. One can either use TCs to produce a reaction network or to directly simulate a system by stochastically sampling and executing the TCs [13, 14]. The method described below involves the latter approach, which provides a substantial advantage when network construction from TCs is computationally expensive.

Here, we suppose that proteins interact through a set of TCs, $\mathbf{T} = \{T_1, \dots, T_M\}$, at rates $\boldsymbol{\eta} = \{\eta_1, \dots, \eta_M\}$. The waiting time τ between two consecutive reaction events follows a Poisson distribution, $p(\tau) = \eta_0 \exp(-\eta_0 \tau)$, where $\eta_0 = \sum_{i=1}^M \eta_i$ is the overall reaction rate in the system. At a given time t , we can apply KMC [15, 16] to determine the time step τ and to sample a specific T_e from the list \mathbf{T} to determine the next reaction event by using the following two formulae:

$$\tau = \frac{\ln(1/\rho_1)}{\eta_0} \quad (1)$$

$$\sum_{i=1}^{e-1} \eta_i < \rho_2 \eta_0 \leq \sum_{i=1}^e \eta_i, \quad (2)$$

where ρ_1 and ρ_2 are uniform random deviates within the interval $(0, 1)$. At each time step, the algorithm requires two computations following the selection of τ and T_e : (1) execute the chosen T_e , and (2) recalculate $\boldsymbol{\eta}$. The former task involves selecting proteins and processing state transitions, which is unambiguous once T_e has been selected, whereas the latter requires consideration of problem-specific details. To execute T_e , one needs to pick out reactant proteins among all proteins that are

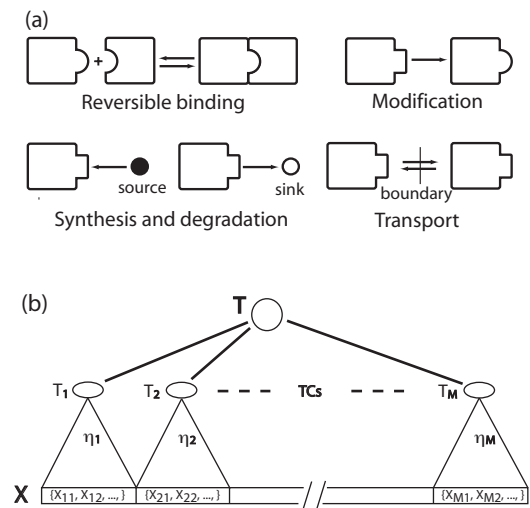


FIG. 1: (a) Graphic illustrations of common TCs for protein-protein interactions including reversible binding, where two molecules interact with each other via complementary domains; post-translational modification, such as phosphorylation or ubiquitination; protein synthesis and degradation, where proteins can be produced, for example, by upregulation of gene expression or broken down by the process of proteolysis; and cross-boundary transport. Note that proteins usually consist of multiple domains and only the one affected by the TC is shown in the figure. (b) Diagrammatic relationship between a system described by TCs and its underlying reaction network. TCs partition the entire reaction list \mathbf{X} into disjoint subsets, where X_{ij} is the j th reaction in partition i . Note that partitions of a reaction network specified by TCs are not necessarily of finite size.

permissive to undergo state transitions specified by T_e . Considering a set of reactant proteins \mathbf{a} , we can describe the joint probability distribution for proteins in set \mathbf{a} to undergo transformation T_e at time $t + \tau$ as

$$P(\mathbf{a}|\tau, T_e) = \frac{c_{\mathbf{a}} \omega_e}{\eta_e}, \quad (3)$$

where ω_e is the rate constant for reactions in class T_e . The coefficient $c_{\mathbf{a}}$ denotes the number of ways proteins can interact with each other. Here, we only consider unimolecular and bimolecular reactions even though the method is not limited to such cases. For instance, if T_e is a unimolecular transformation involving a single protein $\mathbf{a} = \{a\}$, $c_{\mathbf{a}} = m_a$ is a class-specific site multiplicity, e.g., the number of identical sites on protein a that are free to participate in T_e . For a bimolecular transformation, such as association of two proteins $\mathbf{a} = \{a, b\}$, $c_{\mathbf{a}} = m_a m_b$ based on the law of mass action. The coefficient $c_{\mathbf{a}}$ is 0 if all sites are occupied or biochemically blocked, or excluded by model assumptions that constrain application of T_e . The rate of T_e is $\eta_e = u_e \omega_e$, where $u_e = \sum_{\mathbf{a}} c_{\mathbf{a}}$, the total number of distinct ways that proteins can take part in a transformation of type T_e . Based on the above considerations, we can now outline our method as follows.

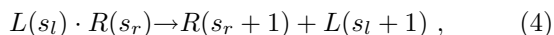
1. Allocate types, copy numbers and initial states of proteins; specify \mathbf{T} and assign rate constants ω ; and initialize η .
2. Sample a time step τ and a class T_e according to the probability distributions indicated in Eqs. (1) and (2).
3. Select interacting proteins according to Eq. (3); update states of the selected proteins; and recalculate η .
4. Repeat step 2 until a stopping criterion is satisfied.

The above steps provide a general procedure for simulating protein interaction systems specified by TCs. A practical implementation of the algorithm, in particular calculations of \mathbf{u} , may be affected by additional constraints imposed on application of TCs.

Algorithm for multivalent ligand-receptor binding

Cell-surface receptor aggregation induced by multivalent ligand-receptor (MLR) binding is an important step in many signal transduction pathways [17]. For example, in the case of basophils and mast cells, complexes of IgE antibody and its receptor FcεRI can recognize multivalent antigens, which leads to aggregation of FcεRI and a cascade of intracellular signaling events [18]. Similar processes, such as macromolecular assembly and viral capsid assembly, play important roles in other biochemical systems [19, 20]. However, modeling the kinetics of MLR binding is difficult because of the combinatorial number of distinct ligand-receptor aggregates that can be generated. In fact, simply enumerating all the possible aggregates is computationally expensive, which prohibits efficient simulation using a method that requires explicit specification of a reaction network. For this reason, most models of MLR interactions are applicable only at thermal equilibrium [21, 22].

Here, we apply the method presented above to study an MLR interaction system that features a highly-branched reaction network. The system has N_l and N_r ligands and receptors, respectively. Each ligand has v_l sites for binding the cell-surface receptor, which has v_r binding sites. All sites on a ligand or a receptor are identical and independent. The system is specified by three TCs using the syntax shown in Table I. For example, T_1 , the ligand-receptor bond dissociation class, is described as



where the left-hand side defines source states of reactants, in this case, the amounts of free sites s_l and s_r on ligand L and receptor R , respectively. The dot between $L(s_l)$ and $R(s_r)$ indicates that L and R are bound to each other. The right-hand side defines the post-transformational states, incremented numbers of free sites on both ligand

and receptor after dissociation. Class T_1 is parameterized by a dissociation rate constant $\omega_1 = k_d$ (Table I).

To compare results with the equilibrium continuum model of Goldstein and Perelson [21], we impose the following constraints on reactions: 1) a ligand cannot associate with a receptor via more than one bond; and 2) a ligand cannot associate with a receptor that is a member of the same aggregate. These constraints prevent the formation of cyclic ligand-receptor complexes, which affects the application conditions of class T_3 and its kinetic rate. In the following, we describe how to select receptors to participate in each TC and the calculation of \mathbf{u} . Related mathematical notations and formulae are summarized in Table I. The source code implementing the simulation procedures is available upon request.

For a T_1 event, the probability of selecting an individual receptor is proportional to its number of bonds. Selecting a particular ligand-receptor pair is performed with a constant-time cost by maintaining a ligand-receptor bond list. The total number of ligand-receptor bonds u_1 is incremented (decremented) with each association (dissociation) event.

For a T_2 event, the probability of a receptor binding a free ligand is proportional to the number of free sites on the receptor. A constant-time operation can be achieved by maintaining a list of all free receptor sites. One can calculate u_2 as the product of the total number of free sites on free ligands, $v_l F_l$, and the total number of free sites on all receptors, $v_r N_r - N_b$.

For a T_3 event, the probability of selecting an individual receptor i is proportional to the product of the number of free sites on the receptor and the number of free ligand sites in other complexes, λ_i . Thus, we maintain a vector $\boldsymbol{\lambda} = (\lambda_1, \dots, \lambda_{N_r})$. A ligand tethered to a receptor on the cell surface is selected according to the number of its free sites. The vector $\boldsymbol{\lambda}$ can be updated iteratively by $\Delta\boldsymbol{\lambda}$ (Table I). Because the constraints on T_3 exclude intra-complex ligand-receptor binding, direct calculation of u_3 involves enumerating all pairwise inter-complex ligand-receptor site combinations, i.e., $u_3 = \sum_{i=1}^{N_c} \sum_j^{i-1} m_i n_j + m_j n_i$, where m_x and n_x are the numbers of free receptor and ligand sites in the x th complex, respectively, and N_c is the total number of ligand-receptor complexes on the cell surface (including free receptors). However, calculation by this approach has a quadratic-time cost. To achieve a linear-time operation, we update u_3 iteratively by Δu_3 , which accounts for the change caused by a reaction event. Calculation of Δu_3 requires different treatments for two types of events (Table I): (i) association or dissociation between two cell-surface complexes, $C[r_\alpha]$ and $C[l_\beta]$; and (ii) free ligand recruitment to or release from receptor complex, $C[r_\alpha]$.

The quantities $m_\alpha, m_\beta, n_\alpha, n_\beta, \Psi_r$ and Ψ_l are calculated by traversing graphs that represent $C[r_\alpha]$ and $C[l_\beta]$ in which the selected receptor r_α and ligand l_β reside at root nodes [30].

TABLE I: Transformation classes for the MLR system

TC	Protocol	ω	\mathbf{u}	$P(\{r\} \tau, T_e)$
T_1 : bond dissociation	$L(s_l) \cdot R(s_r) \rightarrow R(s_r + 1) + L(s_l - 1)$	k_d	N_b	$(v_r - s_r)/N_b$
T_2 : free ligand binding	$L(v_l) + R(s_r > 0) \rightarrow L(v_l - 1) \cdot R(s_r - 1)$	k_{+1}/V	$(v_r N_r - N_b)v_l F_l$	$s_r/(v_r N_r - N_b)$
T_3 : receptor crosslinking	$L(0 < s_l < v_l) + R(s_r > 0) \rightarrow L(s_l - 1) \cdot R(s_r - 1)$	k_{+2}/V	$\sum_{i=1}^{N_r} \lambda_i$	$\lambda_r/\sum_{i=1}^{N_r} \lambda_i$

V , reaction volume; s_r , number of free sites on receptor R ; s_l , number of free sites on ligand L ; F_l , number of free ligands; and N_b , number of ligand-receptor bonds

Calculations of Δu_3 and $\Delta \lambda$ for T_3 .

$$(i) \Delta u_3 = \pm[(m_\alpha n_\beta + m_\beta n_\alpha) + \Psi_r + \Psi_l], \quad \Delta \lambda_i = \begin{cases} \pm(s_{r_\alpha} n_\beta + \Psi_l), & i = \alpha \\ \pm s_{r_i} n_\beta, & r_i \in C[r_\alpha], i \neq \alpha \\ \pm s_{r_i} n_\alpha, & r_i \in C[l_\beta] \\ \pm s_{r_i}, & r_i \notin C[r_\alpha] \cup C[l_\beta] \end{cases}$$

$$(ii) \Delta u_3 = \pm[\Psi_l - (v_l - 1)\Psi_r], \quad \Delta \lambda_i = \begin{cases} \pm \Psi_l, & i = \alpha \\ 0, & r_i \in C[r_\alpha], i \neq \alpha \\ \pm(1 - v_l)s_{r_i}, & r_i \notin C[r_\alpha] \end{cases}$$

(i) association(-)/dissociation(+) between two cell surface complexes, (ii) free ligand recruitment(-)/release(+).

$C[r_\alpha]$: complex contains r_α , $C[l_\beta]$: complex contains l_β .

Ψ_r and Ψ_l : total numbers of free receptor and ligand sites on complexes that are not involved in the event.

m_α and m_β : total numbers of free receptor sites in complex $C[r_\alpha]$ and $C[l_\beta]$, respectively.

n_α and n_β : total numbers of free ligand sites in complex $C[r_\alpha]$ and $C[l_\beta]$, respectively.

III. RESULTS AND DISCUSSION

Figure 2 shows a comparison between stochastic and deterministic simulations. The relaxation kinetics of a bivalent ligand - bivalent receptor system to equilibrium is shown in Fig. 2(a). The deterministic results were obtained by solving a small number of ordinary differential equations (ODEs) as reported in Refs. [23, 24]. The stochastic trajectories recapitulate on average the deterministic solutions. In Fig. 2(b), the equilibrium distribution of receptor aggregates in a bivalent ligand - trivalent receptor system agrees on average with the equilibrium continuum model of Goldstein and Perelson [21].

Average receptor aggregate size provides a gross measure of the degree of ligand-receptor clustering, which can be calculated as $\Gamma = \sum_{n=1}^{N_r} n^2 x_n / N_r$, where x_n is the number of aggregates containing n receptors and $n x_n / N_r$ is the fraction of receptors in aggregates of size n . Figure 3 shows the dependence of mean average aggregate size $\langle \Gamma \rangle$ on the valences v_r and v_l . As v_l and v_r increase, larger aggregates containing more receptors form. The probability of ligand-receptor associations increases with higher receptor and ligand valences, which in turn increases the overall reaction rate, given that other parameters are held fixed. An MLR system with molecules of higher valences also undergoes faster relaxation to equilibrium (results not shown). In particular, the system has higher ligand-receptor association rates η_2 and η_3 for higher v_l and v_r , which moves the system toward having large aggregates that contain more bonds and fewer free sites.

A phase transition in ligand-receptor clustering at equilibrium is predicted by the model of Goldstein and Perelson [21], who showed that finite-sized ligand-receptor complexes can coexist with an infinite-sized polymer-like aggregate (i.e., there is a sol-gel coexistence

regime). Here, by stochastic simulation, we observe significant fluctuations in reaction rates and average aggregate sizes in systems that are parameterized near the boundary of the phase transition. Fluctuation is measured by the coefficient of variation of a random variable x , which is defined as the ratio of the standard deviation to the mean, $\xi_x = \sigma_x / \langle x \rangle$. As shown in Fig. 4(a), the fluctuation of η_3 is more pronounced than η_1 and η_2 at $k_d = 0.01 \text{ s}^{-1}$. Since the vector ω is constant, the rate fluctuations follow the fluctuations of vector \mathbf{u} . Figure 4(b) shows that both u_1 and u_2 change monotonically with k_d , whereas u_3 peaks at an intermediate k_d where the system lies at the edge of the phase transition (cf. Fig 4(d)). In Fig. 4(c), fluctuations of rates follow the same trend, i.e., larger fluctuations caused by smaller combination numbers. The value of ξ_{η_1} increases due to reduced bond number, whereas ξ_{η_2} decreases due to increased free receptor sites, as well as a large free ligand pool when the system equilibrates in the sol phase with a relatively small average aggregate size. The fluctuation in receptor crosslinking rate, ξ_{η_3} , has a minimum at an intermediate value of $\langle \Gamma \rangle$. Moreover, ξ_{η_1} and ξ_{η_3} closely match each other over the range where u_1 and u_3 are proportional to each other. As shown in Fig 4(d), the ‘‘complexity’’ of the system, measured by ξ_Γ , is maximized at the interface of the sol and sol-gel co-existence regions.

We have presented a stochastic simulation method that avoids expanding PPI systems into explicit chemical reaction networks prior to simulation. In this method, systems of interest are specified by transformation protocols that define local state transitions of reactant proteins, and a KMC sampling technique is applied to identify and update protein states such that all chemical species are formed dynamically. For this reason, our method has a computational cost independent of reaction network size.

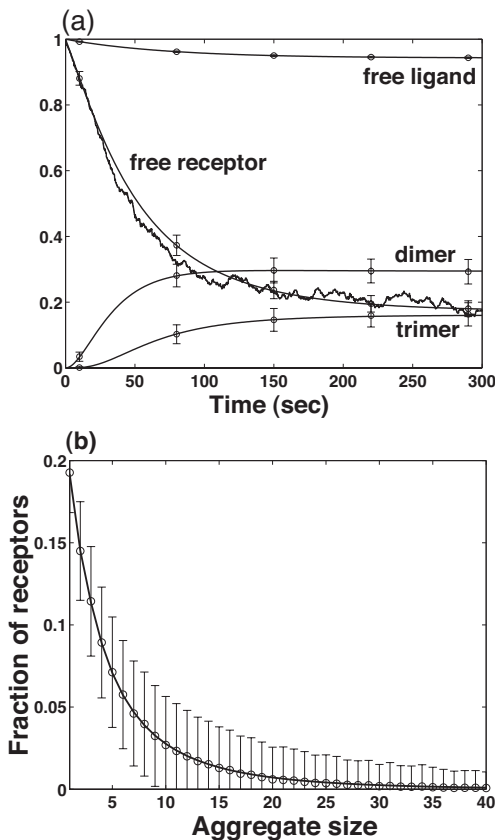


FIG. 2: Computational validation of the simulation algorithm for multivalent ligand-receptor interaction systems. (a) Comparison of normalized results to the ODE solutions for the bivalent ligand and bivalent receptor interaction system. The normalization factor is N_r/n , where n is the number of receptors in an aggregate (e.g., $n = 2$ for dimers, $n = 3$ for trimers, etc.). The means and standard deviations of the simulation results obtained by the simulation method are shown on top of the continuous ODE solutions. One stochastic time trajectory is shown for the free receptor populations. (b) Stochastic receptor aggregate distribution for the trivalent ligand and bivalent receptor system. The system reaches equilibrium after 350 seconds and the averages of equilibrium distributions match the results (solid curve) obtained using the model of Goldstein and Perelson [21]. Parameter values: $N_r = 300$, $N_l = 4200$, $k_{+1} = 6.67 \times 10^{-10}$ nL·s $^{-1}$, $k_{+2} = 100k_{+1}$, $k_d = 0.01$ s $^{-1}$ and $V = 0.001$ nL.

We note that TCs are a set of reaction rules that partition the underlying reaction network into disjoint subsets and also the overall reaction rate η_0 of the system into individual rates for TCs as shown in Fig. 1(b). Rule-based approaches were previously developed to study virus shell assembly [25, 26]. In these studies, rules specifying spatial relationships between binding protein subunits were used to determine virus structures, which provided hypotheses about how viral shell structures arise through specific local interactions. In analogy, TCs specify local relationships between interacting proteins at the resolu-

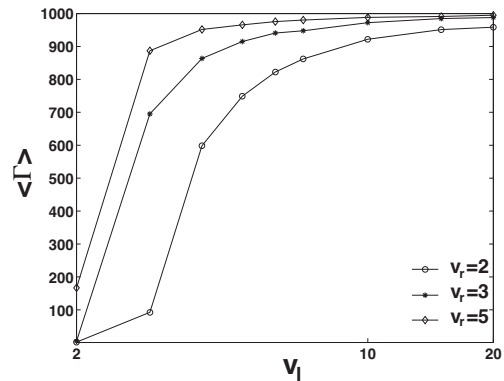


FIG. 3: Relationship between mean average aggregate size $\langle \Gamma \rangle$ and valences of ligand and receptor. $\langle \Gamma \rangle$ is obtained by taking the mean value of Γ over 500 consecutive events at equilibrium. v_l is shown on a log scale. Parameters used are $N_r = N_l = 1000$, $k_{+1} = 6.67 \times 10^{-10}$ nL·s $^{-1}$, $k_{+2} = 100k_{+1}$, $k_d = 0.01$ s $^{-1}$, and $V = 0.001$ nL.

tion of protein domain states, which determine the global dynamics of PPI networks. TCs can be flexibly designed in different ways that equivalently model a given system. Two extreme cases are (1) a single transformation class that characterizes all interactions and (2) an entire chemical reaction network in which each reaction is a distinct transformation class. For a typical PPI system, a practical use of TCs should represent a compromise between these two cases. In particular, as we demonstrated for MLR systems by simulation, systems specified by simple TCs may exhibit complex stochastic behaviors that cannot be efficiently described using chemical reaction networks.

The method presented here was applied to simulate the kinetics of the MLR system where ligands and receptors interact through multivalent binding to form populations of ligand-receptor aggregates. Experimentally testable hypotheses may be formulated based on the simulation results. In particular, significant fluctuations of the average ligand-receptor aggregate size as shown in Fig. 4(d) can be tested for its biological implications. One possibility is that the function of a signaling system may be disrupted in this range because aggregates are unstable, causing the behavior of the system to be uncertain.

The implementation described here is a rejection-free method in which every Monte Carlo step changes the state of the system. The method accounts for the exact TC rates and probability distributions that characterize how reactant molecules undergo transformations. Typically, selecting candidate reactants based on these probability distributions incurs linear-time cost per event scaled by the number of molecules. In alternative null-event implementations of rule-based KMC [14], rates of TCs higher than the exact rates are calculated such that the probability distributions among molecules are uniform (i.e., constant-time molecule selection) or such that

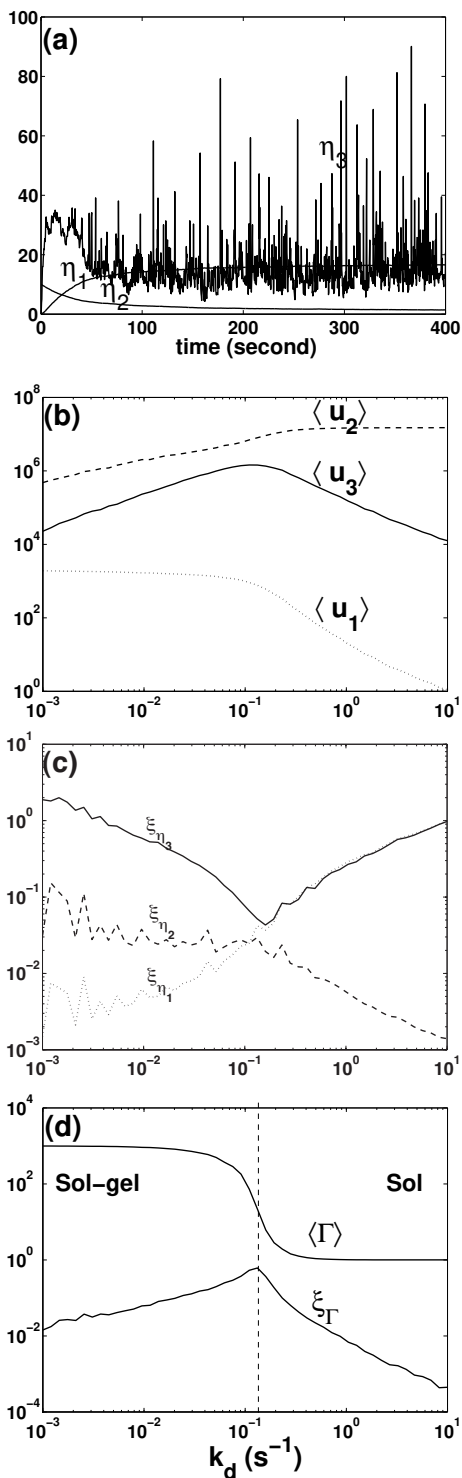


FIG. 4: Rate fluctuations. (a) Time trajectories for the rates of TCs with $k_d = 0.01 \text{ s}^{-1}$. (b) Mean combination numbers. (c) Rate fluctuations. (d) Mean average aggregate size and its fluctuations for different values of k_d . 1000 points were taken after the system reaches equilibrium to calculate the ξ values. $N_r = N_l = 1000$, $v_l = 5$ and $v_r = 3$.

bookkeeping cost are reduced. Simulation advances time but keeps the system configuration unchanged when an identified chemical transformation is determined to be rejected at the time step. Such a simulated event is called a null event. A comparison between rejection-free and null-event methods was briefly discussed by Yang et al. [14], who considered a trivalent ligand and bivalent receptor system. It can be shown that simulations using rejection-free and null-event methods are equivalent in that they both output identical statistical results [27]. We note that there is usually more than one scheme that can be chosen to implement a null-event algorithm. In each scheme, the rate of a TC that can produce null events should be calculated differently. However, the larger the rate, the smaller the time step that can be simulated for each event on average. For the example of the MLR system, a null-event method can be implemented to pick out receptor and ligand (both on the cell surface) based on their numbers of free binding sites available to participate in a reaction of class T_3 . A ligand-receptor pair will be rejected for transformation if they are found to reside in the same complex. In this case, $u_3 = \sum \sum s_r s_l = (v_r N_r - N_b)(v_l(N_l - F_l) - N_b)$. This implementation avoids the need to maintain the λ vector but still incurs a linear cost by traversing graphs of ligand-receptor complexes for a connectivity check. Alternatively, to select a ligand-receptor pair with constant time, one can calculate $u_3 = v_r N_r (v_l - 1)(N_l - F_l)$ to account for the maximal number of free sites on both receptor (v_r) and ligand ($v_l - 1$). A ligand-receptor pair will be rejected for transformation if the receptor and ligand are in the same complex or will be rejected with some probability if either receptor or ligand (or both) has less than the maximal number of free sites. The latter implementation has more rejections per simulated time than the former due to a higher u_3 , which introduces a wider window for null events.

Currently available improvements of Gillespie's method, such as the τ -leap approximation [28], and the next reaction algorithm [29], can be directly applied to our method. For the case of the next reaction algorithm of Gibson and Bruck [29], the reaction dependency graph can be replaced in our method by a dependency graph of TCs, which can then be utilized to determine and recalculate rates of TCs that are affected by a particular event at each step. We note that the next reaction method is useful for simulating large-scale reaction networks in which the dependence between reactions is important for online construction of a compact list of interdependent reactions that are affected by a reaction event. In contrast, TCs are consolidations of reactions, which greatly reduces the sampling space for a Monte Carlo method. Although our method assumes an interaction system is well-mixed (zero dimension in space), it explicitly tracks properties of individual molecules and can be readily extended to incorporate spatial information for a diffusion model.

Acknowledgments

This work was supported by NIH grants GM076570 and RR18754, DOE contract DE-AC52-06NA25396, and

NSFC grant 30870477. J.Y. also acknowledges institutional support. We thank J. R. Faeder and M. I. Monine for helpful discussions.

-
- [1] B. N. Kholodenko, *Nat. Rev. Mol. Cell Biol.* **7**, 165 (2006).
- [2] D. T. Gillespie, *Ann. Rev. Phys. Chem.* **58**, 35 (2007).
- [3] T. Pawson and P. Nash, *Science* **300**, 445 (2003).
- [4] B. Blagoev, S. E. Ong, I. Kratchmarova, and M. Mann, *Nat. Biotechnol.* **22**, 1139 (2004).
- [5] J. V. Olsen, B. Blagoev, F. Gnad, B. Macek, C. Kumar, P. Mortensen, and M. Mann, *Cell* **127**, 635 (2006).
- [6] J. Dengjel, V. Akimov, J. V. Olsen, J. Bunkenborg, M. Mann, B. Blagoev, and J. S. Andersen, *Nat. Biotechnol.* **25**, 566 (2007).
- [7] L. Lok and R. Brent, *Nat. Biotechnol.* **23**, 131 (2005).
- [8] W. S. Hlavacek, J. R. Faeder, M. L. Blinov, R. G. Posner, M. Hucka, and W. Fontana, *Sci. STKE* **2006**, re6 (2006).
- [9] M. L. Blinov, J. Yang, J. R. Faeder, and W. S. Hlavacek, *Lect. Notes Comp. Sci.* **4230**, 89 (2006).
- [10] E. Mjolsness and G. Yosiphon, *Ann. Math. Artif. Intel.* **47**, 329 (2006).
- [11] M. Koschorreck, H. Conzelmann, S. Ebert, and M. Edler, *BMC Bioinformatics* **8**, 336 (2007).
- [12] V. Danos, J. Feret, W. Fontana, R. Harmer, and J. Krivine, *Lect. Notes Comp. Sci.* **4703**, 17 (2007).
- [13] V. Danos, J. Feret, W. Fontana, and J. Krivine, *Lect. Notes Comput. Sci.* **4807**, 139 (2007).
- [14] J. Yang, M. I. Monine, J. R. Faeder, and W. S. Hlavacek, *Phys. Rev. E* **78**, 031910 (2008).
- [15] A. B. Bortz, M. H. Kalos, and J. L. Lebowitz, *J. Comput. Phys* **17**, 10 (1975).
- [16] D. T. Gillespie, *J. Phys. Chem.* **81**, 2340 (1977).
- [17] B. Goldstein, J. R. Faeder, and W. S. Hlavacek, *Nat. Rev. Immunol.* **4**, 445 (2004).
- [18] H. Metzger, *J. Immunol.* **149**, 1477 (1992).
- [19] L. Saiz and J. M. G. Vilar, *Mol. Syst. Biol.* **2** (2006).
- [20] M. Hemberg, S. N. Yaliraki, and M. Barahona, *Biophys. J.* **90**, 3029 (2006).
- [21] B. Goldstein and A. S. Perelson, *Biophys. J.* **45**, 1109 (1984).
- [22] C. Guo and H. Levine, *Biophys. J.* **77**, 2358 (1999).
- [23] A. S. Perelson and C. DeLisi, *Math. Biosci.* **48**, 71 (1980).
- [24] R. G. Posner, C. Wofsy, and B. Goldstein, *Math. Biosci.* **126**, 171 (1995).
- [25] B. Berger, P. W. Shor, L. Tucker-Kellogg, and J. King, *Proc. Natl. Acad. Sci. USA* **91**, 7732 (1994).
- [26] R. Schwartz, P. W. Shor, P. E. Prevelige, and B. Berger, *Biophys. J.* **75**, 2626 (1998).
- [27] A. Chatterjee and D. G. Vlachos, *J. Comput-Aided Mater. Des.* **14**, 253 (2007).
- [28] M. Rathinam, L. R. Petzold, Y. Cao, and D. T. Gillespie, *J. Chem. Phys.* **119**, 12784 (2003).
- [29] M. A. Gibson and J. Bruck, *J. Phys. Chem. A* **104**, 1876 (2000).
- [30] For a ligand-receptor complex C , an acyclic bipartite graph G_c exists implicitly during simulation, in which receptors and ligands are nodes and ligand-receptor bonds are edges. The numbers of receptors and ligands c_r and c_l can be obtained by a linear-time graph traversal of G_c . The number of bonds in C can be calculated as $b = c_r + c_l - 1$, and the number of free receptor and ligand sites can be calculated as $m = v_r c_r - b$ and $n = v_l c_l - b$, respectively. Other quantities can also be calculated by algebraic equations. For example, The number of free receptor sites that are not in C can be calculated as $\Psi_r = v_r N_r - N_b - m$.